Journal of Solid State Chemistry **145,** 557–563 (1999)
Article ID jssc.1999.8217, available online at http://www.idealibrary.com on IDEAL®

An Infrared Spectroscopic Study of the Insulator–Metal Transition and Charge-Ordering in Rare Earth Manganates, $Ln_{1-x}A_xMnO_3$ (Ln = Rare Earth, A = Ca, Sr, Pb)

Anthony Arulraj and C. N. R. Rao[1]

Solid State and Structural Chemistry Unit & CSIR Centre of Excellence in Chemistry, Indian Institute of Science, Bangalore 560012, India

Received September 8, 1998; in revised form February 2, 1999; accepted February 3, 1999

DEDICATED TO PROFESSOR PETER DAY

Infrared absorption spectra of rare earth manganates of the type $La_{0.7}A_{0.3}MnO_3$ (A = Pb, Sr, Ca) show that the compositions which are metallic at room temperature do not exhibit phonon bands, while the insulating compositions show sharp bands. $La_{0.7}Ca_{0.3}MnO_3$ shows some changes in the phonon frequencies across the insulator–metal transition, but more importantly, the temperature variation of the relative band intensities parallels that of the electric resistivity. It appears that infrared absorption in these materials occurs when the resistivity is higher than Mott's maximum metallic resistivity. Infrared absorption spectra of $Nd_{0.5}Ca_{0.5}MnO_3$, $Y_{0.5}Ca_{0.5}MnO_3$, and $Nd_{0.5}Sr_{0.5}MnO_3$ have been investigated through their charge-ordering transition temperatures. The band frequencies increase across the charge-ordering transition accompanied by a significant increase in the band intensities. The stretching and bending bands of the MnO_6 octahedra show splittings in the charge-ordered manganates consistent with the occurrence of octahedral distortion. Some systematics in band frequencies are found with the average radius of A-site cations in $Ln_{0.5}A_{0.5}MnO_3$.

INTRODUCTION

Rare earth manganates of the general formula $Ln_{1-x}A_x MnO_3$ (Ln = rare earth, A = Ca, Sr) have been investigated extensively in the past few years because of the fascinating phenomena and properties they exhibit (1–4). Colossal magnetoresistance in the manganates is one of the important aspects of such investigations. The other equally interesting aspect relates to charge ordering in the manganates, specially favored in certain compositions such as those with $x = 0.5$. While electron transfer from Mn^{3+} to Mn^{4+} by the double-exchange mechanism gives rise to ferromagnetism and metallicity in these manganates, ordering of the Mn^{3+} and Mn^{4+} ions renders them insulating and antiferromagnetic. In the manganates that exhibit a ferromagnetic metallic (FMM) ground state, an insulator to metal transition occurs around ferromagnetic Curie temperature, T_C, on cooling the material. In the insulating state, Jahn–Teller distortion due to the Mn^{3+} ions plays an important role and there is evidence for the presence of Jahn–Teller polarons above T_C (4–6). Colossal magnetoresistance and charge ordering in the manganates are associated with many interesting features. For example, both these phenomena are strongly influenced by the size of the A-site cation. The ferromagnetic T_C in the metallic state increases with the increase in the weighted average radius ($\langle r_A \rangle$) of the A-site cations. The charge ordering transition temperature, T_{CO}, on the other hand, increases with the decrease in $\langle r_A \rangle$. It has been shown that a decrease in $\langle r_A \rangle$ is accompanied by a decrease in the Mn–O–Mn angle in both $Ln_{0.5}A_{0.5}MnO_3$ and $Ln_{0.7}A_{0.3}MnO_3$ compositions. The average Mn–O distance increases slightly with decrease in $\langle r_A \rangle$ in $Ln_{0.5}A_{0.5}MnO_3$ and shows a minimum around 1.24 Å in $Ln_{0.7}A_{0.3}MnO_3$ (7, 8).

In the manganates exhibiting charge ordering, several types of behavior have been observed (8–10). Thus, in the manganates of the composition $Ln_{0.5}A_{0.5}MnO_3$, the charge-ordered (CO) insulating state is transformed to the FMM state, on application of magnetic fields. Such a magnetic-field induced transition occurs only when $\langle r_A \rangle$ is sufficiently large ($\langle r_A \rangle > 1.17$ Å). The manganates with $\langle r_A \rangle < 1.17$ Å are nearly insensitive to magnetic fields. We considered it important to investigate the rare earth manganates by infrared absorption spectroscopy for several reasons. Since in a genuine metallic state, phonon bands do not appear in the infrared absorption spectra because of the screening by the carriers; the intensities of the infrared absorption bands would provide a means to investigate the insulator–metal transition occuring around the ferromagnetic T_C. One would also expect changes in the vibrational band shapes and frequencies across such a transition, since

---

[1] To whom Correspondence should be addressed.

0022-4596/99 $30.00

Jahn–Teller effects would change across the transition. Equally importantly, it should be possible to investigate charge ordering in the manganates in terms of the changes in the infrared band frequencies as well as intensities. In the robust charge-ordered manganates, with low $\langle r_A \rangle$, we would expect the cooperative Jahn–Teller effect to be operative. We report the results of a detailed infrared spectroscopic study on several manganates in this paper. The studies reported in the literature hitherto have by and large been concerned with frequency shifts in the reflectivity and absorption spectra of a few limited compositions of manganates of the type $Ln_{0.7}A_{0.3}MnO_3$ (11, 12). The present investigation includes not only a variable-temperature and composition study of the manganates of the type $Ln_{0.7}A_{0.3}MnO_3$, but also variable temperature studies of several charge-ordered manganates of the composition $Ln_{0.5}A_{0.5}MnO_3$.

EXPERIMENTAL

Polycrystalline samples of $Ln_{0.5}A_{0.5}MnO_3$ were prepared by the conventional ceramic method using appropriate mixtures of oxides and/or carbonates of the constituent elements. The mixtures were first heated at 1473 K in air for 12 h and then ground thoroughly, pelletized, and heated again at 1673 K for 12 h in air. The final heating was done at 1773 K. The $La_{0.7}A_{0.3}Mn_{1-x}Fe_xO_3$ (A = Sr, Pb; $x = 0.00$, 0.03, 0.08) samples were prepared by the decomposition of mixed nitrates. An appropriate mixture of oxides and/or carbonates of the constituent elements was dissolved in nitric acid and the solution was evaporated to dryness. The mixture so obtained was preheated at 773 K in air, pelletized, and heated at 1473 K for 12 h. The $La_{0.7}Sr_{0.3}Mn_{1-x}Fe_xO_3$ samples were given a final heating at 1673 K for 12 h. The Mn^{4+} content in the samples was determined by redox titrations and was generally close to the expected value.

Electrical resistivity measurements were carried out from 300 to 20 K by the four-probe method. The particle size of the sample as well as the heat treatment were such that intergrain effects were minimal. Infrared absorption spectra were recorded with a Bruker IFS 113V FT-IR spectrometer. A Specac variable temperature cell with liquid nitrogen as coolant was used for low temperature studies.

RESULTS AND DISCUSSION

Infrared spectra of the rare earth manganates, $Ln_{1-x}A_xMnO_3$, are characterized by bands due to the stretching mode, ν_s, around 560 cm^{-1} involving the internal motion of the Mn ion against the MnO_6 octahedron and the bending mode, ν_b, around 400 cm^{-1} which is sensitive to the Mn–O–Mn bond angle. A low frequency mode due to the lattice mode, ν_L, occurs around 170 cm^{-1}. Both ν_s and ν_b would be sensitive to octahedral distortion and the associated lowering of symmetry arising from charge-ordering or Jahn–Teller effect. This would result in splitting of these bands. We shall first examine the sensitivity of the infrared absorption spectra to metallicity of the manganates. In order to examine this problem, we have recorded the spectra of orthorhombic $LaMnO_3$, $La_{0.7}Sr_{0.3}MnO_3$ ($T_C = 360$ K), and $La_{0.7}Pb_{0.3}MnO_3$ ($T_C = 330$ K). The last two are metallic at room temperature (~300 K); we compare the spectra of these manganates with those where part of the Mn^{3+} is substituted by Fe^{3+} in order to render them insulating at 300 K, the T_C values having shifted to temperatures below 300 K in the Fe^{3+} substituted compositions (13). The spectrum of insulating $LaMnO_3$ shows the three bands as expected (Fig. 1). There are asymmetric or shoulder-like features in ν_b due to the distorted MnO_6 octahedron. The Sr and Pb substituted metallic samples do not, however, show characteristic absorption bands while the insulating (Fe^{3+}-doped) samples show the presence of the three prominent bands corresponding to the ν_s, ν_b, and ν_L. This simple experiment clearly demonstrates how the infrared absorption spectrum provides a means of following the insulator–metal transition in manganates. It is noteworthy that the bands due to the internal modes in both the Fe^{3+}-substituted $La_{0.7}Sr_{0.3}MnO_3$ and the $La_{0.7}Pb_{0.3}MnO_3$ samples appear as single bands with no evidence for splittings due to octahedral distortion.

We have examined the variable-temperature infrared absorption spectra of a $La_{0.7}Ca_{0.3}MnO_3$ sample which shows

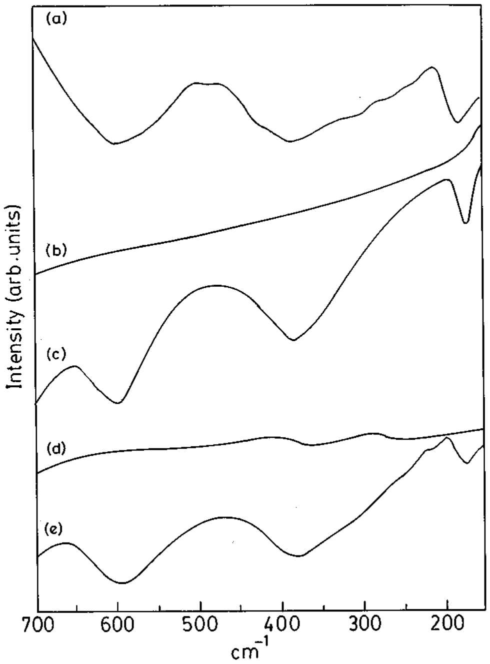

FIG. 1. Infrared spectra of (a) $LaMnO_3$, (b) $La_{0.7}Sr_{0.3}MnO_3$, (c) $La_{0.7}Sr_{0.3}Mn_{0.92}Fe_{0.08}O_3$, (d) $La_{0.7}Pb_{0.3}MnO_3$, (e) $La_{0.7}Pb_{0.3}Mn_{0.97}Fe_{0.03}O_3$.

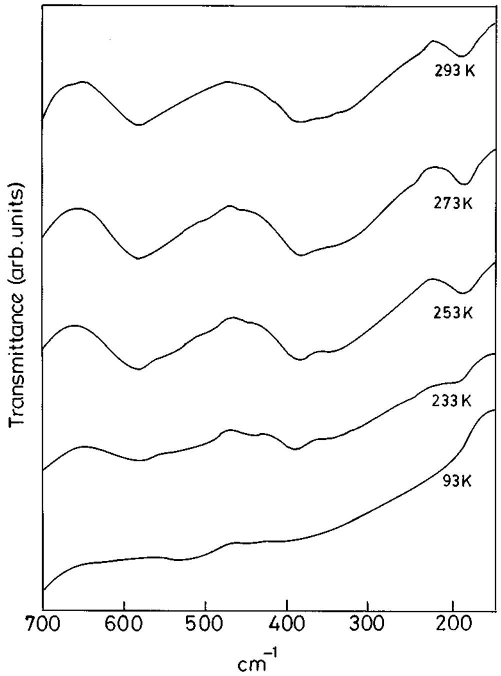

FIG. 2. Variable temperature infrared spectra of $\mathrm{La}_{0.7}\mathrm{Ca}_{0.3}\mathrm{MnO}_3$.

an insulator–metal transition around 263 K as revealed by electrical resistivity measurements. In Fig. 2, we present typical spectra, where we notice a progressive decrease in the band intensities, with a decrease in temperature. In Fig. 3a, we have plotted the relative intensity of ν_s, ν_b, and ν_L bands, I_{rel}, against temperature taking the band height to be unity at 300 K. We see from the figure that the intensities of the stretching, bending modes and the external mode increase on cooling and reach a maximum around 263 K and then decreases on further cooling. The intensities become negligible at low temperatures. The temperature variation of I_{rel} is similar to that of electrical resistivity as can be seen from a comparison of the plots in Figs. 3a and 3b. Thus, the intensities of the infrared bands provide a good measure of the electronic properties of the manganates. The intensity of the band does not abruptly go to zero at the insulator–metal transition, but decreases gradually at $T < T_C$ just as the resistivity. This is significant in that these manganates are not good metals, but metals with a fairly high resistivity (3, 4). In principle one can think of a maximum metallic resistivity, ρ_{max}, corresponding to Mott's minimum metallic conductivity (14, 15), only above which the infrared absorption bands would occur. The resistivities of the manganates in the metallic regime (below T_C) are, in fact, well above the ρ_{max} value of Mott. Consistent with the results on $\mathrm{La}_{0.7}\mathrm{Ca}_{0.3}\mathrm{MnO}_3$ a variable temperature study of the infrared spectra of $\mathrm{La}_{0.7}\mathrm{Pb}_{0.3}\mathrm{MnO}_3$ ($T_C = 330$ K) has shown that above T_C, broad phonon bands appear. There are no discernible bands at room temperature (Fig. 1). In Fig. 4, we show temperature variation of the band frequencies ν_s, ν_b, and ν_L. Both the ν_s and ν_b vibrational frequencies show a small increase below the temperature of the insulator–metal transition (T_C). The lattice mode frequency shows a minimum around this temperature. Such a change in vibrational frequency is expected around T_C since electron–lattice interaction and the Jahn–Teller distortion would be expected to change across the transition. This is

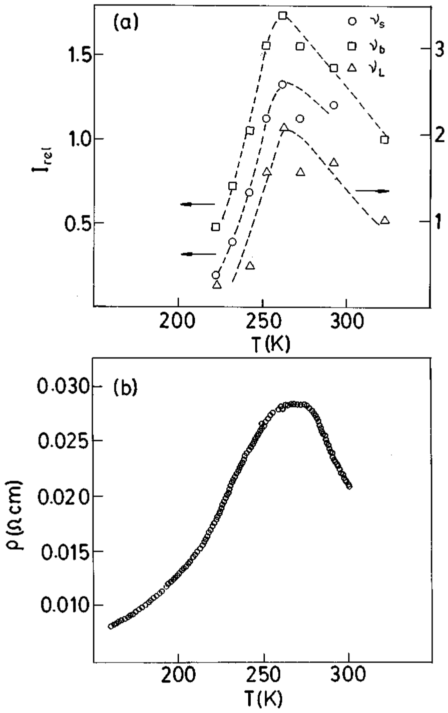

FIG. 3. (a) Temperature variation of the relative intensities of infrared bands of $\mathrm{La}_{0.7}\mathrm{Ca}_{0.3}\mathrm{MnO}_3$. (b) Temperature variation of the electrical resistivity of $\mathrm{La}_{0.7}\mathrm{Ca}_{0.3}\mathrm{MnO}_3$ sample employed for spectroscopic studies.

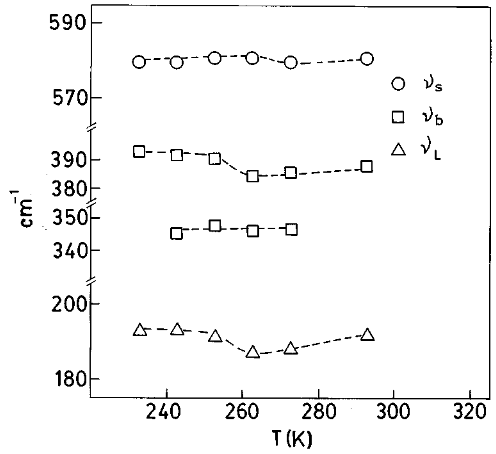

FIG. 4. Temperature variation of the characteristic vibrational frequencies of $\mathrm{La}_{0.7}\mathrm{Ca}_{0.3}\mathrm{MnO}_3$.

particularly true of $La_{0.7}Ca_{0.3}MnO_3$ which has a relatively narrow e_g band and a smaller $\langle r_A \rangle$ compared to $La_{0.7}Sr_{0.3}(Pb_{0.3})MnO_3$. The change in the band frequencies may be taken as a signature of a small polaron to large polaron transition in $La_{0.7}Ca_{0.3}MnO_3$. There is evidence in the literature to show that polarons play an important role in the insulating state, at $T > T_C$ (4–6). It is noteworthy that the bands due to the internal modes, especially ν_b, which appear essentially as single bands in insulating Fe^{3+} substituted $La_{0.7}Sr_{0.3}MnO_3$ and $La_{0.7}Pb_{0.3}MnO_3$ (Fig. 1), show evidence of splitting in $La_{0.7}Ca_{0.3}MnO_3$ with a smaller $\langle r_A \rangle$ (Fig. 2). The splitting signifies the lower symmetry of the MnO_6 octahedra, an aspect which we will examine in some detail in the case of the charge-ordered manganates.

Among the manganates of the composition $Ln_{0.5}A_{0.5}MnO_3$ exhibiting charge-ordering, $Nd_{0.5}Sr_{0.5}MnO_3$ ($\langle r_A \rangle \approx$ 1.24 Å) is unique in the sense that it is in the FMM state around 258 K and becomes charge-ordered at ~150 K (16). CO state is antiferromagnetic (CE type). On application of a magnetic field, the charge-ordered state transforms to the FMM state. We have examined the temperature variation of the infrared spectra of $Nd_{0.5}Sr_{0.5}MnO_3$ in order to study the nature of changes in the absorption bands due to ν_s, ν_b, and ν_L, especially around the charge-ordering transition. We show typical spectra in Fig. 5. We note that the absorption bands are not clearly seen near and above 150 K where the material is in the FMM state. The bands appear distinctly only on cooling below T_{CO}. The bands due to ν_s and ν_b are seen as doubles in the CO state due to the lowered symmetry of the MnO_6 octahedra (Fig. 6). The point group symmetry would be lower than O_h, possibly D_{4h} or C_{4v} (17). We notice small increase in the frequency of the ν_s and ν_b bands across T_{CO}, but we have not plotted the data above T_{CO} in Fig. 6 due to uncertainty in fixing the positions of these weak bands. The splitting of the bending mode increases as the temperature is lowered. The ν_s and ν_b doublets can, in principle, be assigned to the $Mn^{3+}O_6$ and $Mn^{4+}O_6$ octahedra which become distinct in the CO state. We do not prefer such an assignment because there could be considerable vibrational coupling. In Fig. 7, we show plots of the relative intensities of the ν_s and ν_b bands against temperature. The plots show an increase in I_{rel} around T_{CO}. The

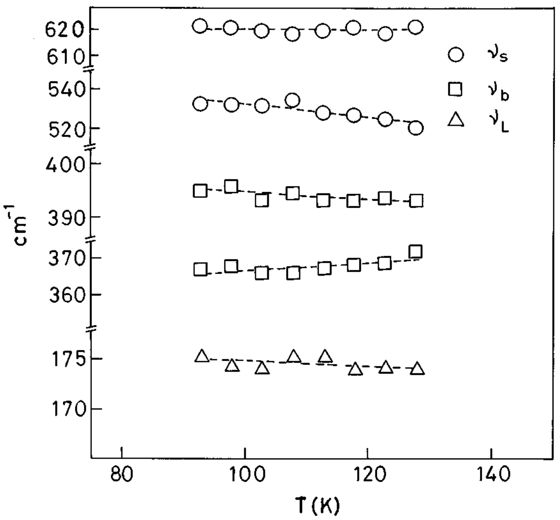

FIG. 6. Temperature variation of the characteristics vibrational frequencies of $Nd_{0.5}Sr_{0.5}MnO_3$. The band positions above 130 K have not been shown because of the uncertainty in fixing exact positions of the weak intensity bands. There was, however, a discernible decrease in the frequencies at $T \geq 140$ *K*.

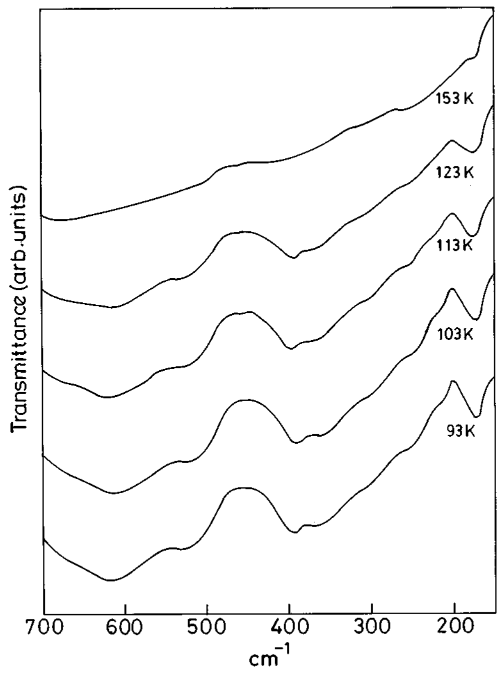

FIG. 5. Variable temperature infrared spectra of $Nd_{0.5}Sr_{0.5}MnO_3$.

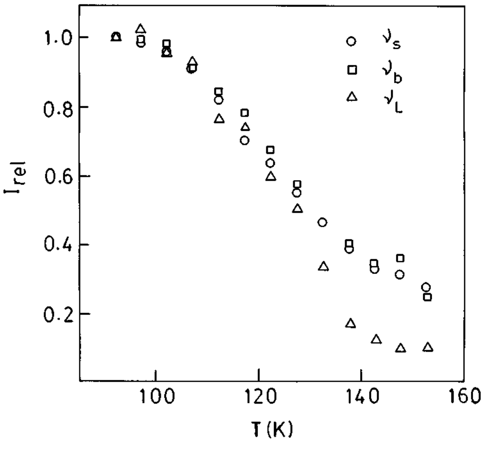

FIG. 7. Temperature variation of the relative band intensities of $Nd_{0.5}Sr_{0.5}MnO_3$. Intensities of the split bands were taken to be the average of the heights of the two peaks.

increase in the band intensity on cooling below T_{CO} is consistent with the localized electron behavior in the insulating CO phase. The variation in the intensity of the external mode shows evidence for charge-ordering features even better than ν_s and ν_b (Fig. 7).

In contrast to the behavior of $\mathrm{Nd_{0.5}Sr_{0.5}MnO_3}$, $\mathrm{Nd_{0.5}Ca_{0.5}MnO_3}$ as well as $\mathrm{Y_{0.5}Ca_{0.5}MnO_3}$, with much smaller $\langle r_A \rangle$, do not exhibit the FMM state at any temperature and are charge-ordered even at relatively high temperatures, with the charge-ordering temperature, T_{CO}, in the range 220–260 K (8, 9). The CO state transforms to a metallic state on the application of very high magnetic fields in the case of $\mathrm{Nd_{0.5}Ca_{0.5}MnO_3}$ ($\langle r_A \rangle = 1.17$ Å). Magnetic fields have no effect on the CO state of $\mathrm{Y_{0.5}Ca_{0.5}MnO_3}$ ($\langle r_A \rangle = 1.13$ Å). In Fig. 8, we show the variable temperature infrared spectra of $\mathrm{Nd_{0.5}Ca_{0.5}MnO_3}$. Distinct phonon bands appear in the entire temperature range, the only change being the decrease in intensity with increase in temperature. The spectra show a distinct doublet due to ν_s at low temperatures, particularly below 240 K. This material is known to show a charge-ordering transition around 220 K (8, 18) and this would cause octahedral distortion. There are some changes in the frequencies of ν_s, ν_b, and ν_L around this temperature (Fig. 9). The most distinct change is in the lattice mode frequency which shows a marked decrease below the charge-ordering transition. The ν_s and ν_b mode frequencies are generally higher in the charge-ordered state. The relative intensities of ν_s and ν_b bands show an increase around T_{CO} (Fig. 10), just as in $\mathrm{Nd_{0.5}Sr_{0.5}MnO_3}$. A preliminary study of charge-ordered $\mathrm{Pr_{0.7}Ca_{0.3}MnO_3}$ also showed an increase in the relative intensities of the three bands below T_{CO}, indicating that this behavior is characteristic of the changes near T_{CO}. This is consistent with the increase in resistivity below T_{CO}.

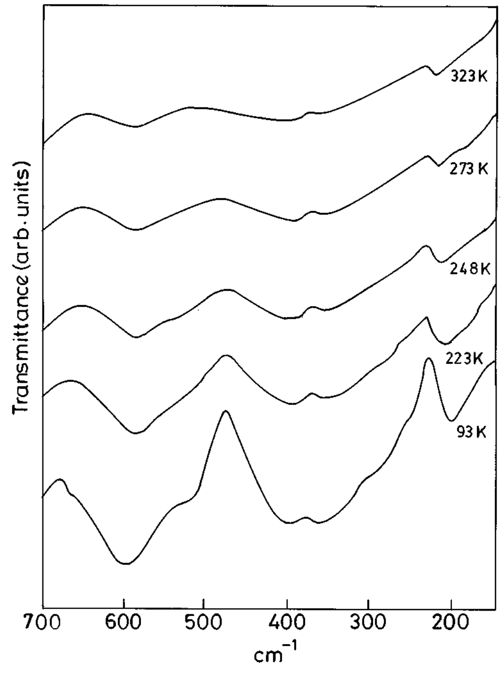

FIG. 8. Variable temperature infrared spectra of $\mathrm{Nd_{0.5}Ca_{0.5}MnO_3}$.

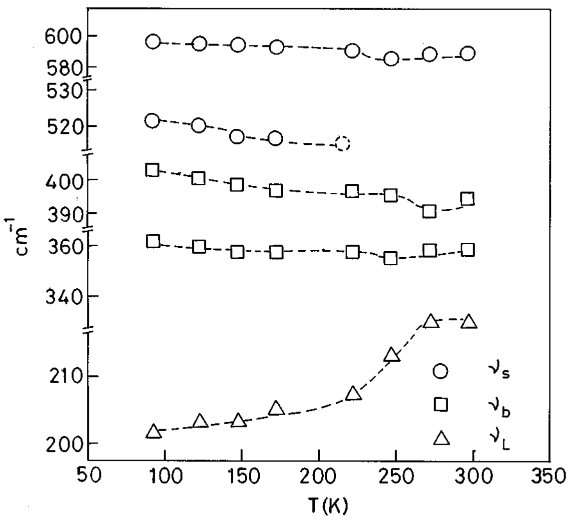

FIG. 9. Temperature variation of the characteristic vibrational frequencies of $\mathrm{Nd_{0.5}Ca_{0.5}MnO_3}$.

In Fig. 11, we show the variable temperature infrared spectra of $\mathrm{Y_{0.5}Ca_{0.5}MnO_3}$. The band due to ν_s appears as a triplet rather than a doublet in this manganate. The same is true of the band due to ν_b. The charge-ordered state in this manganate is robust because of the very small $\langle r_A \rangle$ (1.13 Å) and effects due to Jahn–Teller distortion would be maximum. The lattice distortion is also highest in $\mathrm{Y_{0.5}Ca_{0.5}MnO_3}$ reaching 1.82% at low temperatures (8, 9). The splitting of ν_s and ν_b bands is therefore not surprising since it reflects the magnitude of departure of octahedral

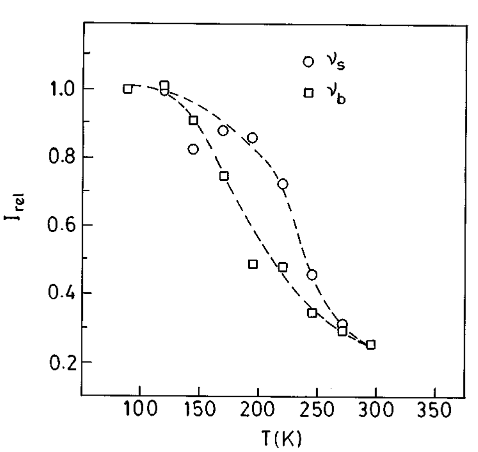

FIG. 10. Temperature variation of the relative band intensities of $\mathrm{Nd_{0.5}Ca_{0.5}MnO_3}$.

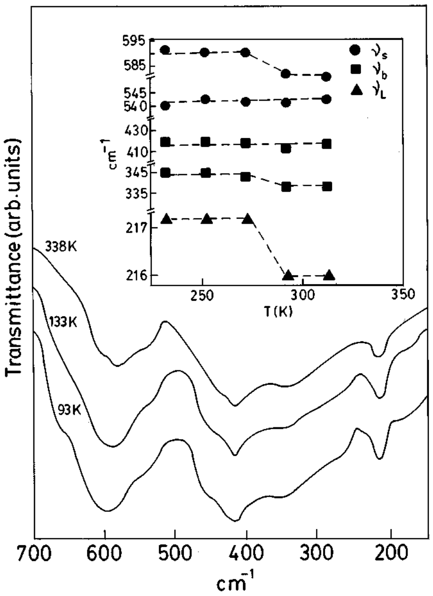

FIG. 11. Variable temperature infrared spectra of $Y_{0.5}Ca_{0.5}MnO_3$. In the inset, the variation of the characteristic frequencies of $Y_{0.5}Ca_{0.5}MnO_3$ near T_{CO} is shown.

symmetry (17). The charge-ordered transition in this manganate is around 260 K. There is a definitive increase in the absorption frequencies at temperatures below T_{CO} (see inset of Fig. 11). It is somewhat surprising that the ν_L mode frequency is higher in the CO state of this manganate compared to $Nd_{0.5}Ca_{0.5}MnO_3$. The relative intensities of ν_s and ν_b bands increase below T_{CO}.

It has been shown recently that the average Mn–O distance in $Ln_{0.5}A_{0.5}MnO_3$ increases while the Mn–O–Mn angle decreases with a decrease in $\langle r_A \rangle$ (19). The increase in the Mn–O distance with $\langle r_A \rangle$ is about 0.02 Å, in the $\langle r_A \rangle$ range of 1.12–1.24 Å. The Mn–O–Mn angle, however, varies significantly, decreasing from 175° to about 150° in this range of $\langle r_A \rangle$. The decrease in the Mn–O–Mn angle is expected to decrease the Mn–Mn transfer integral. We would therefore expect some variation in the vibrational frequencies of $Ln_{0.5}A_{0.5}MnO_3$ with $\langle r_A \rangle$. An increase in the Mn–O distance (with decrease in $\langle r_A \rangle$) should decrease ν_s while the accompanying decrease in the Mn–O–Mn angle should increase ν_b. With such changes in structure, there would be changes in the local symmetry as well. In Fig. 12, we show the variation in the ν_s and ν_b band frequencies. There is a slight decrease in frequency of ν_s with an increase in $\langle r_A \rangle$. The highest bending frequency in the manganates shows a decrease with an increase in $\langle r_A \rangle$. More exactly, the splitting of the bending band increases with a decrease in $\langle r_A \rangle$ or in the Mn–O–Mn angle. As mentioned earlier, in $Y_{0.5}Ca_{0.5}MnO_3$, with the smallest $\langle r_A \rangle$, the deformation band is a triplet, just as the stretching band, due to the low symmetry of the octahedron. At such small $\langle r_A \rangle$, the cooperative Jahn–Teller effect and associated distortions become prominent.

CONCLUSIONS

Infrared spectra of rare earth manganates of the type $Ln_{0.7}A_{0.3}MnO_3$ which undergo insulator–metal transitions around the ferromagnetic Curie temperature (due to the double-exchange process) have been investigated across the insulator–metal transition brought about by compositional changes or temperature. Phonon band intensities decrease markedly in the metallic phase and the frequencies show some changes across the temperature-induced transition.

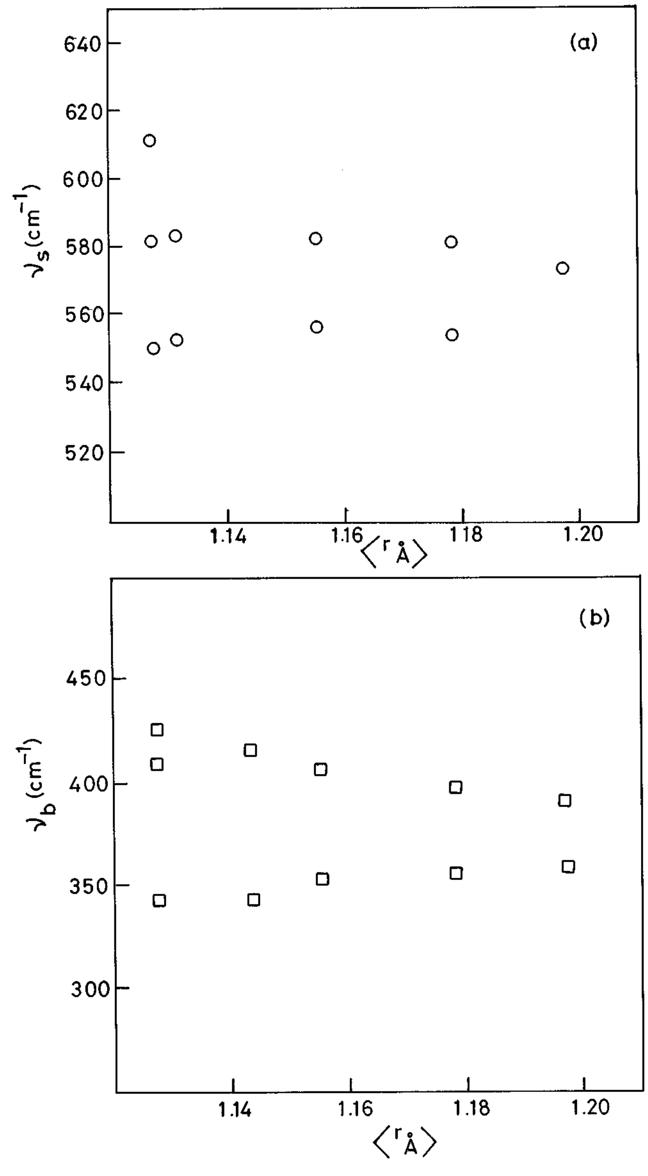

FIG. 12. Variation of vibrational frequencies of $Ln_{0.5}Ca_{0.5}MnO_3$ with $\langle r_A \rangle$.

That there are infrared absorption bands at all in the so-called metallic phases of some of these materials is related to their relatively high resistivities (higher than that permitted by the Mott criterion). Thus, the temperature-variation of the phonon intensities of $\mathrm{La}_{0.7}\mathrm{Ca}_{0.3}\mathrm{MnO}_3$ parallels that of the electrical resistivity.

Charge-ordered manganates of the type $Ln_{0.5}A_{0.5}\mathrm{MnO}_3$ show an increase in the band frequencies around the charge-ordering transition, accompanied by a significant increase in the intensities, the latter being consistent with the increase in resistivity below the transition. At low temperatures, these materials show extensive band splittings due to octahedral distortion arising from the Jahn–Teller effect.

ACKNOWLEDGMENTS

The authors thank the Science Office of the European Commission for support of this research. A. A thanks CSIR, India, for the Senior Research Fellowship. They acknowledge Dr. Sugantha for the samples of the Sr- and Pb-substituted manganates in Fig. 1.

REFERENCES

1. Y. Tokura, *Current Opinion Solid State Mater. Sci.* **3,** 175 (1998).
2. A. P. Rameriz, *J. Phys.: Condens. Matter* **9,** 8171 (1997).
3. C. N. R. Rao and A. K. Cheetham, *Adv. Mater.* **9,** 1009 (1997).
4. C. N. R. Rao and A. K. Raychaudhuri *in* "Colossal Magnetoresistance, Charge Ordering and Related Properties of Manganese Oxide" (C. N. R. Rao and B. Raveau (Eds.), World Scientific, Singapore, 1998.
5. J. L. Garcia-Munoz, M. Suaaidi, J. Fontcuberta, and J. Rodriguez-Carvajal, *Phys. Rev. B* **55,** 34 (1997).
6. A. J. Millis, *Phys. Rev. B* **53,** 8434 (1996).
7. P. G. Radaelli, G. Iannone, M. Marezio, H. Y. Hwang, S-W. Cheong, J. D. Jorgensen, and D. N. Argyriou, *Phys. Rev. B* **56,** 8265 (1997).
8. A. Arulraj, P. N. Santhosh, R. Srinivasa Gopalan, Ayan Guha, A. K. Raychaudhuri, N. Kumar, and C. N. R. Rao, *J. Phys.: Condens. Matter.* **10,** 8497 (1998).
9. A. Arulraj, R. Gundakaram, A. Biswas, N. Gayathri, A. K. Raychaudhuri and C. N. R. Rao, *J. Phys.: Condens. Matter* **10,** 4447 (1998).
10. C. N. R. Rao and A. K. Cheetham, *Science* **276,** 911 (1997).
11. K. H. Kim, J. Y. Gu, H. S. Choi, G. W. Park, and T. W. Noh, *Phys. Rev. Lett.* **77,** 1877 (1996).
12. L. Kebin, L. Xijun, Z. Kaigui, Z. Jingsheng, and Z. Yuheng, *J. Appl. Phys.* **81,** 6943 (1997).
13. M. Suganthа, R. S. Singh, A. Guha, A. K. Raychaudhuri, and C. N. R. Rao, *Mat. Res. Bull.* **33**, 1129 (1998).
14. N. F. Mott, *Phil. Mag.* **26,** 1015 (1972).
15. C. N. R. Rao and P. Ganguly *in* "The Metallic and Non Metallic State of Matter" (P. P. Edwards and C. N. R. Rao, Eds.), Taylor and Francis, London, 1985.
16. H. Kuwahara, Y. Tomioka, A. Asamitsu, Y. Moritomo, and Y. Tokura, *Science* **270,** 961 (1995).
17. C. N. R. Rao, Indian *J. Pure. Appl. Phys.* **16,** 277 (1978).
18. T. Vogt, A. K. Cheetham, R. Mahendiran, A. K. Raychaudhuri, R. Mahesh, and C. N. R. Rao, *Phys. Rev. B* **54,** 15303 (1996).
19. C. N. R. Rao, A. Arulraj, P. N. Santhosh, and A. K. Cheetham, *Chem. Mater.* **10,** 2714 (1998).